

Modeling the phase behavior of cyclic compounds in mixtures of water, alcohols and hydrocarbons

T.M. Soria, F.A. Sánchez, S. Pereda*, S.B. Bottini

Planta Piloto de Ingeniería Química, PLAPIQUI, CONICET, Universidad Nacional del Sur, UNS Camino La Carrindanga Km 7–CC: 717, Bahía Blanca, Argentina



ARTICLE INFO

Article history:

Received 7 August 2013

Received in revised form 7 October 2013

Accepted 13 October 2013

Available online 21 October 2013

Keywords:

Cycloalkane

Cycloalcohol

GCA-EoS

Equation of state

VLE and LLE

ABSTRACT

In this work the GCA-EoS model is applied to represent the phase behavior of systems containing cyclic hydrocarbons, alcohols and water. The presence of naphthenic hydrocarbons in normal fossil fuels makes this information important for the prediction of properties of bioethanol/gasoline blends. Since GCA-EoS is a group contribution equation of state, also cyclo-alcohols were included in the study to increase the experimental databank for tuning the model parameters. The GCA-EoS was able to correlate and predict the phase behavior of multicomponent mixtures typical of bioethanol/gasoline blends.

© 2013 Elsevier B.V. All rights reserved.

1. Introduction

Cycloalkanes are present in significant amounts in fossil fuels, along with normal and branched paraffins and aromatic hydrocarbons. Cyclic and polycyclic structures of hydrocarbons and oxygenated derivatives are also present in other natural products such as terpenes and steroids.

Cycloalkanes have properties similar to those of normal alkanes, although they have higher densities, boiling and melting points. The geometry of cycloalkanes originates different degrees of angle strain. The carbon atoms in these compounds are sp^3 hybridized and therefore deviate from the ideal tetrahedral bond angles of 109°. Ring strain is highest for cyclopropane, in which the carbon atoms have 60° C–C bond angles, decreases in cyclobutane and cyclopentane, and is negligible in cyclohexane where the folding of the ring allows ideal tetrahedral bond angles to be achieved [1].

The mixtures of non-polar cycloalkanes with associating alcohol and water molecules are highly non-ideal. Even though association models based on Wertheim's theory [2] have been widely used to represent the phase behavior of mixtures of *n*-alkanes with water and alcohols, only a limited number of papers in the literature deal with similar cycloalkane mixtures. Different versions of the SAFT model have been used to represent vapor–liquid and liquid–liquid equilibria of binary mixtures of cyclohexane and ethylcyclohexane with water and alcohols [3–8]. Also, the cubic-plus-association

(CPA) equation and the Nonrandom Hydrogen Bonding (NRHB) theory have been applied to represent the phase equilibria of binary mixtures of cyclohexane, ethyl- and *n*-butyl-cyclohexane with alcohols and water [9–14]. In all these works only cycloalkanes with 6 carbon atoms in the ring have been considered.

In the present work a more systematic study on cycloalkanes, including rings with different number of carbon atoms, was undertaken. The group contribution with association equation of state (GCA-EoS) was used to calculate the phase behavior of mixtures of these cycloalkanes with alkanes, water and alcohols. Cyclic alcohols were also included in the study.

Even though the characteristic functional group of alkanes and cycloalkanes is the methylene group (CH_2), the differences found in the structure of cycloalkane rings suggest that it would be necessary to introduce a distinction among them.

2. Thermodynamic model: GCA-EoS

The GCA-EoS model [15,16] is an extension to associating compounds of the GC-EoS equation of state first proposed by Skjold-Jørgensen [17]. The original model is based on the generalized van der Waals partition function and the group contribution principle. There are three different contributions to the residual Helmholtz energy in the GCA-EoS model: repulsive, attractive and associative.

The Carnahan–Starling repulsive term follows the expression developed by Mansoori and Leland [18] for mixtures of hard spheres. It is a function of the critical hard sphere diameter d_c , characteristic of the pure-compound molecular size, and has no binary

* Corresponding author. Tel.: +54 291 4861700; fax: +54 291 4861600.

E-mail addresses: spereda@plapiqui.edu.ar, spereda@gmail.com (S. Pereda).

or higher-order parameters. The attractive term is a group contribution version of the NRTL expression, with density-dependent mixing rules. The attractive energy between like groups is calculated from pure group parameters: the number of surface segments (q) and the energy per segment (g). This last parameter is temperature dependent, being g^* , g' and g'' the constants of the energy temperature dependence. Binary parameters are introduced to quantify interactions between unlike groups i and j : the asymmetric, temperature independent, non-randomness parameters α_{ij} and α_{ji} , and the symmetric, temperature dependent, binary interaction parameters, represented by the constants k_{ij}^* and k_{ij}' . Finally, the association term is a group contribution version of the association theory proposed by Wertheim [2]. Each associating functional group is characterized by the energy ε and volume κ of association. More details on the model equations and parameters are given elsewhere [19,20] and summarized in the Appendix.

It should be mentioned that the GCA-EoS model reduces to the original GC-EoS equation when applied to non-associating systems. Hence, the parameters of non-associating functional groups, like the methylene group, should have the same values in both models.

3. Characterization of cyclic functional groups

Cycloalkanes are represented in the original GC-EoS equation, by the so-called cyclic alkane functional groups (cyCH₂ and cyCH). The surface segments of these two groups are equal to those of the corresponding alkane groups (CH₂ and CH). These values were taken from Bondi [21], as it is done in the UNIFAC model. The energy parameters ($g^* = 466\,550 \text{ atm cm}^6 \text{ mol}^{-2}$; $g' = -0.6062$; $g'' = 0$), the same for cyCH₂ and cyCH groups, were obtained by Skjold-Jørgensen [17] regressing the vapor pressures of cyclohexane and methylcyclohexane. When the GC-EoS is applied to predict the vapor pressure of cycloalkanes other than cyclohexane and methylcyclohexane using the original parameters presented by Skjold-Jørgensen [17], large errors are found. In order to find the reason for this discrepancy, the effect of the geometry of cycloalkanes in the q value of the cyCH₂ group was investigated. Ab initio calculations were performed to obtain the molecular structure and the carbon–carbon bond angles of cycloalkane molecules with 4 up to 8 carbon atoms in the ring. For this purpose the GAMESS software [22] was run to get the structure of minimum configurational energy for each compound. Table 1 reports the results of these calculations and shows that the predicted angle of cyclic alkanes increases from cyclobutane to cyclooctane. The angle of the tetrahedral bond corresponding to the structure of linear alkanes is also included for comparison.

Following Bondi [21], it becomes clear that q increases as the C–C–C bond angle decreases. The results of Table 1 for cycloalkanes indicate that there is not a single q for the cyCH₂ group and that its value should decrease with the number of carbon atoms in the ring.

Assuming that the original energy parameters per surface segment of all cycloalkanes remain the same as reported by Skjold-Jørgensen ($g^* = 466\,550 \text{ atm cm}^6 \text{ mol}^{-2}$; $g' = -0.6062$; $g'' = 0$), the van der Waals relative area (A_{vdw}), of cyclobutane, cyclopentane and cyclooctane (molecules with the same value of all C–C–C bond angles) were obtained by adjusting the vapor pressures of the pure components. As shown in Fig. 1, the surface area of these three cycloalkane molecules is well represented by the following linear dependence with the number of carbon atoms (CN) in the ring:

$$A_{vdw} = 0.4593 \times CN + 0.506 \quad (1)$$

Eq. (1) allows the straightforward prediction of the surface area of other cycloalkanes not included in the parameterization procedure, like shown with cross symbols in Fig. 1 for cyclic propane, heptane, nonane and decane.

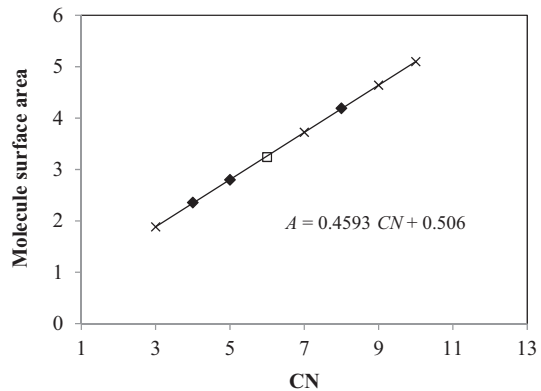


Fig. 1. Van der Waals relative areas of cycloalkanes: (♦) values derived from vapor pressure data [23]; (□) relative area of cyclohexane obtained as $6 \times q_{\text{CH}_2}$ of *n*-alkanes; (×) values predicted from Eq. (1).

From Eq. (1) we can derive a simple relation to predict the q value of the cyCH₂ group in any cycloalkane molecule containing CN carbon atoms in the ring:

$$q(\text{CH}_2) = 0.4593 + \frac{0.506}{CN} \quad (2)$$

With the purpose of representing phase equilibrium properties of alkyl-cycloalkanes, two new groups (CH₃cyCH and CH₂cyCH) were defined in this work. The methyl-cyclopentane molecule, for instance, would be represented by 4 (cyCH₂)₅ + 1 (CH₃cyCH)₅ groups and the ethyl-cyclohexane molecule by 5 (cyCH₂)₆ + 1 (CH₂cyCH)₆ + 1 CH₃ groups.

To determine the parameters of these new CH₃cyCH and CH₂cyCH functional groups, the results obtained for the non-substituted cycloalkanes were taken as a basis. According to the GAMESS software, the C–C–C bond angles in the ring are not significantly affected by the presence of the paraffinic chains. The CH₃cyCH and CH₂cyCH groups were considered to have the same values of the energy parameters, but different q values, depending on the number of carbon atoms in the ring. For instance, the number of surface segments of the CH₃cyCH group in the methyl cyclopentane molecule is calculated as:

$$q(\text{CH}_3\text{cyCH})_5 = q(\text{CH}_3) + q(\text{cyCH})_5 = q(\text{CH}_3) + q(\text{cyCH}_2)_5 - 0.312 \quad (3)$$

where $q(\text{CH}_3)$ is the number of surface segments of the CH₃ alkane group ($q = 0.848$), $q(\text{cyCH}_2)_5$ is obtained from Eq. (2) for $CN = 5$ and 0.312 represents the difference between the surface segments of the CH₂ and CH alkane groups, due to the extra covalent bond in the first one. This difference should be applied to calculate $q(\text{cyCH})_{CN}$ from the corresponding $q(\text{cyCH}_2)_{CN}$, for any number of carbon atoms. That is, for any value of CN :

$$q(\text{cyCH}_2)_{CN} - q(\text{cyCH})_{CN} = q(\text{CH}_2) - q(\text{CH}) = 0.312 \quad (4)$$

The final energy parameters listed in Table 2 for the (CH₃cyCH)_{CN} and (CH₂cyCH)_{CN} groups were then obtained regressing the vapor pressures of methylcyclopentane and 1,4-dimethylcyclohexane.

In summary, for any value of CN , the (CH₃cyCH)_{CN} and (CH₂cyCH)_{CN} groups are essentially the same functional group, having the same value of the energy per segment (g), but different number of surface segments (q) available for group interactions. The same is valid for the set of (cyCH₂)_{CN} and (cyCH)_{CN} groups. The importance of this approach is that no binary interaction parameters are required to correct the attractive energy, because they are considered the same group. Moreover, no binary parameters are necessary to quantify the interactions between the different paraffin groups present in normal-, branched- and cyclo-alkanes.

Table 1

Structure and C—C—C angles of alkane and cycloalkane molecules. Van der Waals molecular area A_{vdW} and group surface area q are reported in the last columns.

Cycloalkane	Structure (Optimized using GAMESS software)	C—C—C angles	q	A_{vdW}
n-Alkane		$(CN - 2) \times 109.5^\circ \pm 0.05^\circ$ (ideal angle for tetrahedral bond)	$q_{CH_2, Bondi} = 0.540$ $q_{CH_3, Bondi} = 0.848$	$(CN - 2) \times 0.540 + 2 \times 0.848$
Cyclobutane		$4 \times 88^\circ \pm 0.3^\circ$	$q_{88} = 0.589$	2.356
Cyclopentane		$5 \times 104^\circ \pm 2^\circ$	$q_{104} = 0.560$	2.800
Cyclohexane		$6 \times 111^\circ \pm 0.2^\circ$ (closer to 109.5° , ideal angle)	$q_{CH_2} = 0.540$ (CH_2 of n-alkanes)	$6 \times q_{CH_2} = 3.240$
Cycloheptane		$5 \times 114^\circ \pm 0.3^\circ$ and $2 \times 117.6^\circ$	$A_{vdw}/7 = q = 0.532$	From Eq. (1) = 3.721
Cyclooctane		$8 \times 115^\circ \pm 0.3^\circ$	$q_{115} = 0.524$	4.192

This, of course, increases the predictive capacity of the GCA-EoS model.

Cycloalcohols were also studied in this work. The current version of the GCA-EoS equation has been applied only to normal and branched alkanols, characterized through the CH_2OH and $CHOH$ functional groups. To include cyclic alcohols, a new $cyCHOH$ group was defined, with the hydroxyl group bonded to a cyclic carbon. The first step to characterize this functional group was to determine its

surface area. Based on the results obtained for cycloalkanes, the hypothesis adopted here was, once again, to make the number of surface segments of the $cyCHOH$ group dependent on the number of carbon atoms in the ring.

The contribution of the hydroxyl subgroup to the surface area was first calculated from the difference between the q values of the CH_2OH and CH_2 groups reported by Skjold-Jørgensen [17]:

$$q(OH) = q(CH_2OH) - q(CH_2) = 1.124 - 0.540 = 0.584 \quad (5)$$

and the $(cyCH)_{CN}$ contribution to q was determined by applying the same relation used for substituted cycloalkanes. Then:

$$q(cyCHOH)_{CN} = q(OH) + q(cyCH)_{CN} \quad (6)$$

Following the same approach applied to cyclic alkanes, all $(cyCHOH)_{CN}$ groups are considered to share the same values of the energy parameters. The next step is then to calculate the values of these parameters by adjusting appropriate experimental data. In this case it should be taken into account that the alcohol molecules have two types of groups: the polar and associating $(cyCHOH)_{CN}$ group and the non-polar $(cyCH_2)_{CN}$ groups. Hence, binary interaction parameters will most likely be required to quantify dispersive forces between these two groups and also association effects will have to be included. The hypothesis here was to make the association parameters of the new $(cyCHOH)_{CN}$ group equal to those of the CH_2OH and $CHOH$ groups in alkanols (energy = 2758.8 K and volume = $0.8709 \text{ cm}^3 \text{ mol}^{-1}$) [24] and the non-randomness parameters equal to zero. The energy parameters of the $(cyCHOH)_{CN}$ group and the binary interaction parameters (k_{ij}^* and k'_{ij}) between this group and $(cyCH_2)_{CN}$ and $(CH_3cyCH)_{CN}$ were determined by simultaneous regression of the vapor pressure of cyclohexanol and methylcyclohexanol [23] and vapor–liquid equilibrium data for the cyclohexane + cyclohexanol system [25]. These parameters are reported in Tables 2 and 3, together with the remaining parameters determined in this work. The temperature T^* , in the first column of Table 2 represents the reference temperature of each functional group. Following the original GC-EoS equation [17], the

Table 2
GCA-EoS pure group parameters of cyclic groups.

Group	T^*/K	q_i	$g_{ii}^{*}/\text{atm cm}^6 \text{ mol}^2$	g'_{ii}	g''_{ii}
$(cyCH_2)_{C4}$	600.0	0.589	466550	-0.6062	0
$(cyCH_2)_{C5}$	600.0	0.560			
$(cyCH_2)_{C6}$	600.0	0.540			
$(cyCH_2)_{C7}$	600.0	0.532			
$(cyCH_2)_{C8}$	600.0	0.524			
$(CH_3cyCH)_{C5}$	600.0	1.096	365430	-0.7670	0
$(CH_3cyCH)_{C6}$	600.0	1.076			
$(CH_2cyCH)_{C5}$	600.0	0.788			
$(CH_2cyCH)_{C6}$	600.0	0.768			
$(cyCHOH)_{C5}$	512.6	0.833	738325	-0.6405	0.1565
$(cyCHOH)_{C6}$	512.6	0.812			
$(cyCHOH)_{C7}$	512.6	0.804			
$(cyCHOH)_{C8}$	512.6	0.796			

Table 3

GCA-EoS binary interaction parameters of attractive term.

Group <i>i</i>	Group <i>j</i>	k_{ij}^*	k'_{ij}	α_{ij}	α_{ji}	Experimental data and source
H ₂ O	CH ₃ cyCH	1.000	0	1	1.2	LLE H ₂ O + 2, 3 and 4 m-cyC ₆ ol [26]
	cyCH ₂	1.008	0	2	0	LLE H ₂ O + cyC ₅ ol, cyC ₆ ol, cyC ₇ ol and cyC ₈ ol [26]
	cyCHOH	1	0	0	0	LLE H ₂ O + cyC ₅ ol, cyC ₆ ol, cyC ₇ ol and cyC ₈ ol [26]
	CH ₃ cyCH [∞]	0.820	-0.150	0	1.2	LLE H ₂ O + m- and dm-cyC ₆ [27–29]
	CH ₂ cyCH [∞]	1.000	-0.110	4	4.5	LLE H ₂ O + ethylcyC ₆ [27–30]
	cyCH ₂ [∞]	0.740	-0.170	0	1.8	LLE H ₂ O + cyC ₅ , cyC ₆ , cyC ₇ and cyC ₈ [29,31]
CH ₃ OH	CH ₃ cyCH	0.985	-0.035	0	10.5	LLE CH ₃ OH + m-cyC ₅ and m-cyC ₆ [32]
	cyCH ₂	0.983	0.025	0	15	LLE CH ₃ OH + cyC ₅ and cyC ₆ [32–34]
C ₂ H ₅ OH	CH ₃ cyCH	0.970	-0.038	0	0	VLE C ₂ H ₅ OH + m-cyC ₆ [35,36]
	cyCH ₂	0.931	-0.063	2	0	VLE C ₂ H ₅ OH + cyC ₆ [37,38] LLE C ₂ H ₅ OH + cyC ₆ + H ₂ O [39,40]
CH ₂ OH	CH ₃ cyCH	0.955	-0.078	0	0	VLE propanol + m-cyC ₆ [41]
	cyCH ₂	0.940	-0.004	0	0	VLE propanol, butanol, hexanol and decanol + cyC ₆ [25,42–45]
cyCHOH	cyCH ₂	0.880	-0.060	0	0	p ^{vap} cyC ₆ ol [23]
	CH ₃ cyCH	0.941	-0.114	0	0	VLE cyC ₆ ol + cyC ₆ [25] p ^{vap} m-cyC ₆ ol [23]

m: methyl, dm: dimethyl, ol: alcohol.

typical values of 600 K and 512.6 K were adopted for cycloalkanes and cycloalcohols, respectively.

It is important to highlight again that groups having the same values of the surface energy g , will have the same values of the binary interaction parameters, which extends the predictive capacity of the GCA-EoS model.

4. Results and discussion

4.1. Vapor pressure of cyclic compounds

As it was already mentioned, the repulsive term in the group-contribution equation of state is a Carnahan–Starling equation for hard spheres of diameter d . By applying the equation of state and the physical constraints ($\partial P/\partial V = \partial^2 P/\partial V^2 = 0$) at the critical point, Skjold-Jørgensen [17] found the relation between the critical hard sphere diameter d_c and the critical properties of non-associating substances ($d_c = (0.08943RT_c/P_c)^{1/3}$). In order to improve the performance of the equation of state and/or to obtain a value of d_c when there is no information on the critical properties of a given substance, Skjold-Jørgensen [17] proposed to obtain the d_c value by fitting the equation to a certain point of the vapor pressure curve (d_c^b). Contrary to the critical diameter derived from the critical properties of the pure component (d_c^c), the values of d_c^b will

depend on the model parameters and will not represent exactly the critical point. The difference between the d_c^c and d_c^b values gives a good insight on the suitability of the parameterization procedure being applied. Of course, the better the predictive capacity of the equation, the closer the d_c^b and d_c^c will be.

Table 4 compares the vapor pressures of pure cycloalkanes calculated using a single value for the surface area of the cyCH₂ and cyCH groups, as done by Skjold-Jørgensen [17], with those obtained by applying the different surface areas reported in **Table 2** of this work. In both cases the calculations were performed by using both, d_c^c and d_c^b . A reduced temperature range from 0.5 to 0.95 was covered. From the results reported in **Table 4** it becomes clear that: (i) the vapor pressures predicted using the d_c^c and q proposed by Skjold-Jørgensen show very high percentage deviations ($\Delta P\%$); (ii) the values of d_c^b required to decrease these errors are quite different from those of d_c^c ; (iii) the use of different q for the cyclic paraffin groups, as proposed in this work, reduces the $\Delta P\%$ deviations and, consequently, makes the d_c^b values quite close to d_c^c . These results will also have an effect on the prediction of liquid–liquid equilibria (LLE). As shown in previous work [20,24], the value of the critical diameter has a direct impact on the LLE predictions. In order to achieve good predictions of both, vapor–liquid and liquid–liquid equilibria using the same set of parameters, the value of the critical diameter should be as close

Table 4
Relative deviations ($\Delta P\%$) in the prediction of cycloalkane vapor pressures by GCA-EoS, using critical diameters at the critical point (d_c^c) or the normal boiling point (d_c^b) conditions. Reduced temperature range = 0.5–0.95. Critical diameter units (cm mol^{-1}).

Compound	$d_c^c(T_c, P_c)$	Original parameters			This work		
		$\Delta P\%(d_c^c)$	d_c^b	$\Delta P\%(d_c^b)$	$\Delta P\%(d_c^c)$	d_c^b	$\Delta P\%(d_c^b)$
Cyclopropane [*]	3.7661	791	3.3542	3.11	6.22	3.7582	6.3
Cyclobutane	4.0949	221	3.8296	0.22	3.76	4.0889	4.56
Cyclopentane	4.3857	72.4	4.2638	1.60	3.84	4.3830	3.70
Cyclohexane	4.6556	3.23	4.6646	3.22	3.23	4.6646	3.22
Cycloheptane [*]	4.8993	21.6	4.9652	3.23	2.45	4.9089	3.10
Cyclo-octane [*]	5.1322	38.5	5.2609	3.64	3.75	5.1414	4.20
Cyclononane [*]	5.3424	64.2	5.5710	14.47	16.2	5.3805	9.87
Cyclodecane [*]	5.5031	71.8	5.8439	3.50	28.9	5.5933	5.81
Methylcyclopentane	4.7104	58.0	4.6020	1.49	6.90	4.7272	4.30
Methylcyclohexane	4.9628	3.10	4.9741	3.28	7.82	4.9882	3.20
t-1,4-Dimethylcyhexane	5.2973	16.6	5.2628	5.15	4.67	5.2938	3.74
t-1,2-Dimethylcyhexane [*]	5.3233	44.0	5.2308	9.0	28.4	5.2620	4.5
t-1,3-Dimethylcyhexane [*]	5.3288	53.0	5.2227	6.3	36.3	5.2538	4.4
t-1,2-Dimethylcypentane [*]	4.9240	5.0	4.9180	2.7	21.0	4.9873	2.75
t-1,3-Dimethylcypentane [*]	4.9240	4.0	4.9190	2.7	21.3	4.9884	2.66

* Predictions.

Table 5

GCA-EoS correlation and prediction of cyclic alcohol vapor pressures.

Compound	T_c	T_r	$\Delta P\%$	$d_c^b/\text{cm mol}^{-1}$
Cyclopentanol*	619.5	0.53–0.93	3.81	4.571
Cyclohexanol	650.10	0.50–0.84	4.93	4.795
Cycloheptanol*	653.15	0.55–0.88	3.63	5.043
Cyclooctanol*	666.15	0.50–0.85	3.79	5.403
t-2-Methylcyclohexanol	617.0	0.57–0.88	5.60	5.158
t-3-Methylcyclohexanol	627.0	0.54–0.90	4.30	5.099
t-4-Methylcyclohexanol	622.0	0.60–0.90	5.60	5.124

* Predictions.

as possible to the one that reproduces the critical point and its constraints.

Fig. 2 shows the correlated and predicted vapor pressures of cycloalkanes (solid and dashed lines, respectively), including alkyl-substituted cycloalkanes.

Also the vapor pressures of cyclic alcohols were calculated. Table 5 summarizes the relative deviations obtained in the given range of reduced temperatures (T_r); also the d_c^b of each cyclic alcohol is reported. Some of the results are graphically shown in Fig. 3.

4.2. Phase equilibria of binary mixtures including cyclic compounds

Following the general criteria applied in previous work [19,20,24], the GCA-EoS model is used employing the same set of parameters to represent different types of equilibria (VLE, LLE, SLE) in a wide range of temperatures and pressures. For this purpose, a databank with more than 1400 experimental data points, covering a temperature and pressure range of 273–560 K and 10⁻² to 100 bars, respectively, was set in order to fit the model parameters and to test its predictive capacity with those datasets not included in the parameterization step.

Tables 2 and 3 report the values of pure group and binary interaction parameters obtained in this work for cyclic compounds. Table 3 also includes the type and source of experimental data used in the parameterization process.

It should be noted that Table 3 reports specific interaction parameters for groups defined as cyCH_2^∞ , $\text{CH}_3\text{cyCH}^\infty$ and $\text{CH}_2\text{cyCH}^\infty$. As in the case of paraffins and aromatic hydrocarbons

[19,20,24], these parameters should be used in any application of the model requiring highly accurate predictions of the low mutual solubilities between water and cycloalkanes.

Tables 6 and 7 summarize the results achieved in the correlation and prediction of the phase equilibrium conditions of all the binary systems with cyclic compounds studied in this work. The tables include information about the range of temperature T and pressure P covered by the experimental data, the number N of data points and its source. For VLE calculations the tables report the average relative deviations in the vapor phase composition (Δy) and the deviations (Δz) in pressure (isothermal data) or in the liquid phase composition (isobaric data). For LLE calculations the errors are reported as average absolute deviations and average relative deviations (between brackets) in the mutual solubilities.

One of the main objectives of this work was to represent the phase equilibrium conditions of gasoline/ethanol blends. In general cyclohexane is used as the typical cycloparaffin present in reformates. Therefore, the binary system ethanol + cyclohexane is a relevant system to study. Fig. 4 shows the results of vapor–liquid equilibrium calculations for this binary system in the temperature range 273–338 K. It can be seen that the model correlates and predicts the experimental data with high accuracy. GCA-EoS is able to follow precisely the increase in ethanol azeotropic composition with temperature. On the other hand, Fig. 5 shows the correlation of the mutual solubility between different cycloalkanes and methanol at atmospheric pressure. The model achieves a good correlation for all compounds, except for cyclopentane, whose data are close to the upper critical solution temperature.

Fig. 6 shows the mutual solubility between water and various cycloalkanes. The prediction of these data is of utmost importance for evaluating the water tolerance of fuel blends and the environmental impact in case of a gasoline spill. As it is the case with alkanes and aromatic hydrocarbons [19,20,24], GCA-EoS is able to predict,

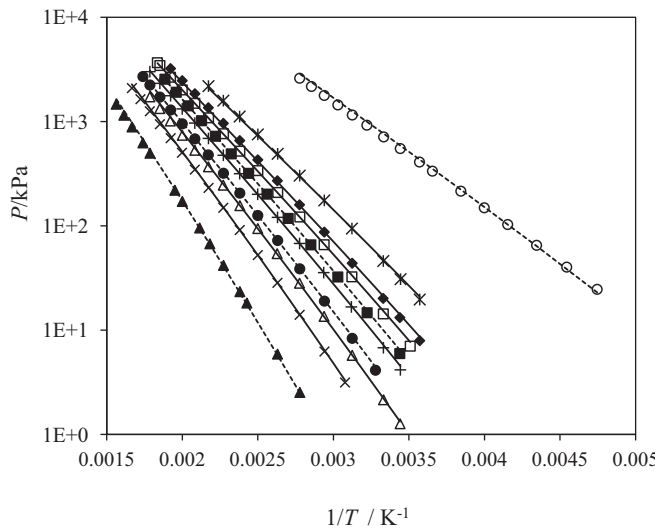


Fig. 2. Cycloalkane vapor pressures. Experimental data [23]: (○) cyclopropane, (*) cyclopentane, (◆) methylcyclopentane, (□) cyclohexane, (■) t-1,2-dimethylcyclopentane, (+) methylcyclohexane, (●) cycloheptane, (Δ) t-1,4-dimethylcyclohexane, (×) cyclooctane, (▲) cyclodecane. Solid and dashed lines: GCA-EoS correlations and predictions, respectively.

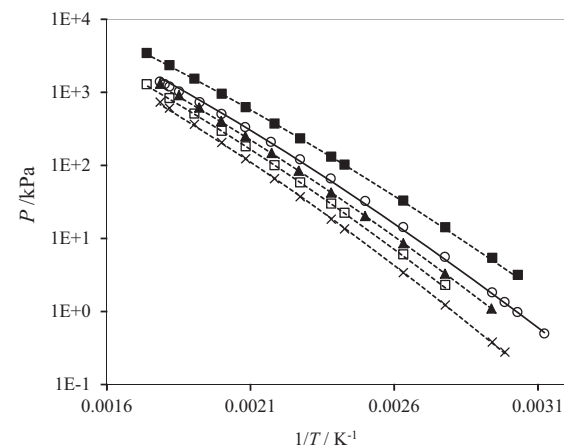


Fig. 3. Cyclic alcohol vapor pressures. Experimental data [23]: (■) cyclopentanol, (○) cyclohexanol, (▲) t-4-methylcyclohexanol, (□) cycloheptanol, (×) cyclooctanol. Solid and dashed lines: GCA-EoS correlations and predictions, respectively.

Table 6
VLE and LLE binary systems: GCA-EoS correlations.

Compound		T/K	P/kPa	$\Delta z\%^a$	$\Delta y_1\%^b$	N	Source
1	2						
<i>Vapor–liquid equilibria</i>							
Alcohols + Cycloalkanes							
Ethanol	cyC ₆	273, 340	3–101	4.10	2.80	19	[37,38]
	m-cyC ₆	273, 328	2–51	3.15	4.50	27	[35,36]
1-propanol	cyC ₆	347–370	101	2.10	4.32	41	[42]
	cyC ₆	328, 338	18–73	0.97	2.10	31	[43]
	m-cyC ₆	360–366	101	1.97	4.02	11	[41]
1-butanol	cyC ₆	308	6–21	3.80	1.30	13	[44]
1-hexanol	cyC ₆	290–363	9	3.31	3.23	17	[45]
1-decanol	cyC ₆	298	1.5–13	4.95	0.21	11	[44]
cyC ₆ ol	cyC ₆	308, 318, 328	14–43	3.60	0.08	32	[25]
<i>Liquid–liquid equilibria</i>							
Alcohols (A) + Cycloalkanes (HC)							
Methanol	cyC ₅	273–290	101	A in HC $3 \times 10^{-2} (12)$	HC in A $1.3 \times 10^{-1} (33)$	14	[32]
	cyC ₆	288–313	101	$4 \times 10^{-2} (29)$	$1.1 \times 10^{-2} (6)$	12	[32–34]
	m-cyC ₅	277–304	101	$4.4 \times 10^{-2} (16.5)$	$8 \times 10^{-3} (3.8)$	17	[32]
	m-cyC ₆	278–313	101	–	$1.6 \times 10^{-2} (11)$	8	[32]
Water (W) + Cycloalcohols (A)							
Water	cyC ₅ ol	273–364	101	A in W $3.7 \times 10^{-4} (16)$	W in A $2.8 \times 10^{-2} (5)$	18	[26]
	cyC ₆ ol	273–364	101	$3.7 \times 10^{-3} (13)$	$1.4 \times 10^{-2} (3)$	20	[26]
	3-m-cyC ₆ ol	273–364	101	$4.5 \times 10^{-4} (22)$	$1.7 \times 10^{-2} (5.5)$	20	[26]
	4-m-cyC ₆ ol	273–364	101	$3.5 \times 10^{-4} (16)$	$3.9 \times 10^{-2} (10)$	20	[26]
Water (W) + Cycloalkanes (HC)							
Water	cyC ₅	278–471	101	HC in W $2.7 \times 10^{-4} (24)$	W in HC $3.5 \times 10^{-4} (45)$	15	[31]
	cyC ₆	278–482	101	$4.2 \times 10^{-5} (23)$	$5.2 \times 10^{-3} (22)$	24	[31]
	cyC ₇	298–303	101	$1.2 \times 10^{-6} (21)$	$9.6 \times 10^{-6} (2.1)$	2	[31]
	cyC ₈	274–313	101	$2.3 \times 10^{-7} (25)$	–	9	[29]
	m-cyC ₆	299–446	101	$2.1 \times 10^{-6} (12)$	$6.7 \times 10^{-3} (28)$	19	[27]
	1,2-c-dm-cyC ₆	274–444	101	$8.6 \times 10^{-7} (22)$	$4.2 \times 10^{-3} (23)$	19	[28,29]
	1,2-t-dm-cyC ₆	274–443	101	$4.1 \times 10^{-7} (24)$	–	13	[28,29]
	Ethyl cyC ₆	274–560	10–9930	$1.1 \times 10^{-4} (23)$	$7.2 \times 10^{-2} (25)$	30	[27–30]

Compounds nomenclature: cy = cyclo, m = methyl, dm = dimethyl, c = cis, t = trans, ol = alcohol.

AAD = average absolute deviation, ARD% = percent relative average deviation.

^a $\Delta z\% = \text{ARD}\%$ in pressure for isothermal data or in liquid phase composition for isobaric data.

^b $\Delta y\% = \text{ARD}\%$ in vapor phase composition.

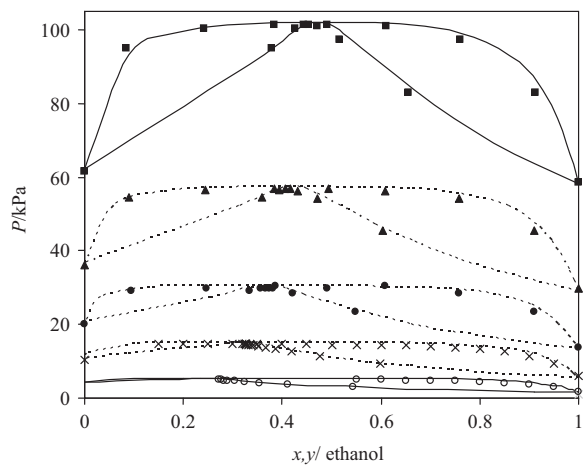


Fig. 4. Vapor–liquid equilibria of ethanol + cyclohexane. Experimental data [37,56,57]: (○) 273.15 K, (×) 293.15 K, (●) 308.15 K, (▲) 323.15, (■) 338.15 K. Solid and dashed lines: GCA-EoS correlations and predictions, respectively.

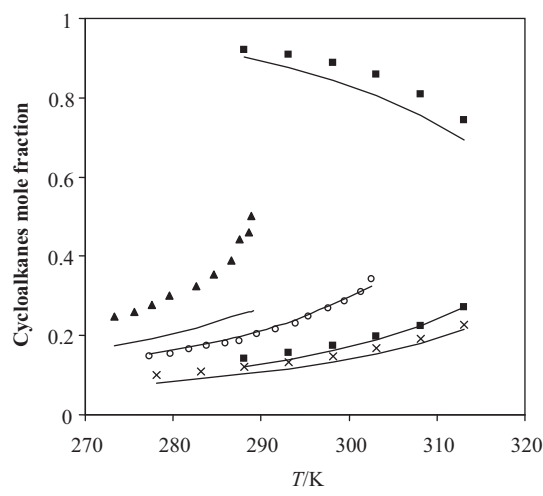


Fig. 5. Solubility of cycloalkanes in methanol. Experimental data [32–34]: (▲) cyclopentane, (○) methylcyclopentane, (■) cyclohexane, (×) methylcyclohexane. Solid lines: GCA-EoS correlations. The upper line and dots correspond to the solubility of methanol in cyclohexane.

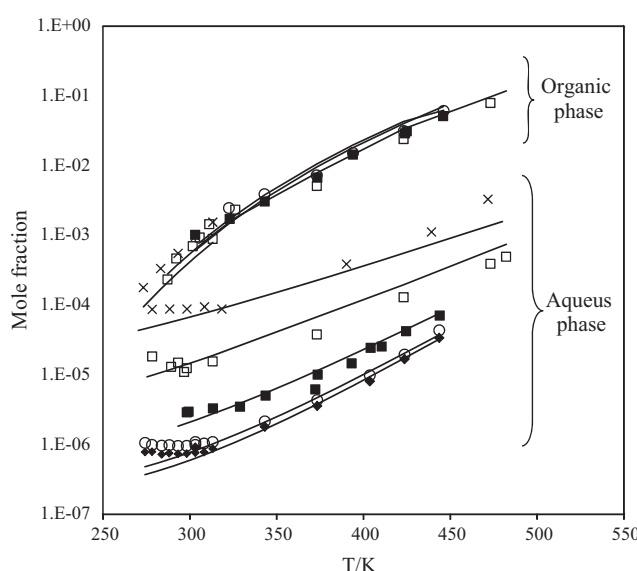
Table 7

VLE and LLE binary systems: GCA-EoS predictions.

Compound	T/K	P/kPa	$\Delta z\%$ ^a	$\Delta y_1\%$ ^b	N	Source
1	2					
<i>Vapor–liquid equilibria</i>						
Paraffins + cycloalkanes						
Pentane	cyC ₆	312–353	101	0.19	1.43	28
	m-cyC ₅	309–343	101	0.42	0.95	44
Hexane	cyC ₆	343–352	101	3.19	5.42	16
	cyC ₆	343	77–101	1.01	0.79	7
	m-cyC ₅	342–345	101	0.091	0.21	11
Heptane	cyC ₆	354–370	101	0.21	0.37	13
	cyC ₆	313, 333	14–49	1.67	1.41	11
Octane	cyC ₆	298, 328	4–41	2.82	1.71	16
Alcohols + cycloalkanes						
Methanol	cyC ₆	293, 318, 328	10–104	4.50	5.01	42
	cyC ₆	327–332	101	6.50	1.70	17
	m-cyC ₅	333–324	99	4.80	5.30	5
Ethanol	cyC ₆	314–343	40, 101	4.44	4.34	40
	cyC ₆	298, 308, 323	9.5–57	1.80	2.62	33
	cyC ₅	323, 373	96–530	3.22	1.43	14
	m-cyC ₆	283, 293, 308	4–20	1.85	5.10	46
	m-cyC ₅	333–350	101	1.73	3.40	13
cyC ₆ ol	cyC ₆	298	2–13	4.60	0.63	23
	cyC ₅	298	10–43	6.10	0.44	19
cyC ₅ ol	cyC ₅	298	12–42	4.70	0.40	14
	cyC ₆	298	3–13	3.20	1.46	20
cyC ₇ ol	cyC ₇	298	0.70–3	2.06	0.082	18
<i>Liquid–liquid Equilibria</i>						
Cycloalcohols (A) + Water (W)						
cyC ₇ ol	Water	273–364	101	A in W 3.4×10^{-4} (12)	W in A 1.5×10^{-2} (4.2)	20
cyC ₈ ol	Water	283–364	101	–	1.5×10^{-2} (5.5)	18
Water (W) + Cycloalkanes (HC)						
Water	ethyl-cyC ₅	283–303	101	HC in W –	W in HC 4.6×10^{-5} (6.1)	3
Water	butyl-cyC ₅	283–303	101	–	9.8×10^{-5} (14.2)	3

Compounds nomenclature: cy = cyclo, m = methyl, dm = dimethyl, c = cis, t = trans, ol = alcohol.

AAD = average absolute deviation, ARD% = percent relative average deviation.

^a $\Delta z\% = \text{ARD}\%$ in pressure for isothermal data or in liquid phase composition for isobaric data.^b $\Delta y\% = \text{ARD}\%$ in vapor phase composition.**Fig. 6.** Water + cycloalkane mutual solubility. Experimental data [27–29,31]: (x) cyclopentane, (□) cyclohexane, (●) cyclo-octane, (○) methylcyclohexane, (○) c-1,2-dimethylcyclohexane, (◆) t-1,2-dimethylcyclohexane. Solid lines: GCA-EoS correlations.

by group contribution and using a single set of parameters, the significant difference between the solubility of each cycloparaffin in water, while keeping nearly constant the water composition in the hydrocarbon phase. However, in this case the model under-predicts the temperature at which the cycloparaffins show minimum solubility in water.

Even though GCA-EoS is used under a group contribution approach (i.e. the same parameters for the same functional groups), Fig. 6 shows that the model is able to distinguish the difference between two configurational isomers: cis-1,2-dimethylcyclohexane and trans-1,2-dimethylcyclohexane. This difference is resolved by the GCA-EoS repulsive term, through the value of the critical diameter of each isomer.

The last family of binary systems studied was the water + cyclo-alcohol mixtures. Similarly to water + cycloalkane binary systems, the solubility of cyclo-alcohols in the aqueous phase decreases as the molecular weight of the alcohol increases. Fig. 7 shows the good results obtained in the correlation and prediction of mutual solubilities. In this case GCA-EoS is able to describe the minimum in solubility.

4.3. Phase equilibria of ternary systems including cyclic compounds

A large amount of experimental data on the ethanol + water + cyclohexane ternary system is available in the literature [39,40,64–67]. Ternary mixtures of *n*-hexane,

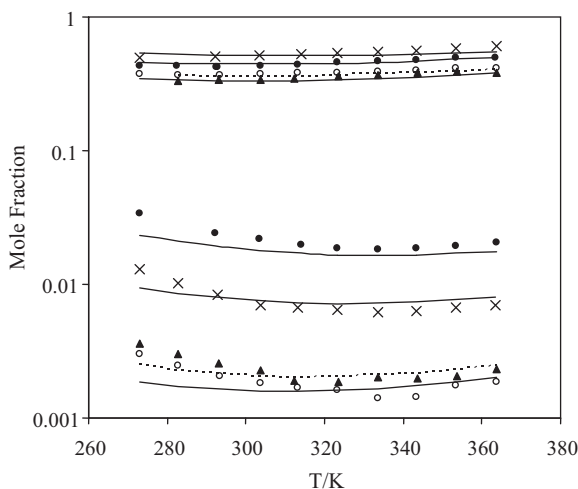


Fig. 7. Liquid-liquid equilibria of water + cyclo-alcohol binary systems. Experimental data [26]: (●) cyclopentanol, (×) cyclohexanol, (▲) cycloheptanol, (○) 1,4-dimethylcyclohexanol. Solid and dashed lines: GCA-EoS correlations and predictions, respectively.

isoctane and cyclohexane with ethanol and water constitute key systems for studying the phase behavior of gasoline/bioethanol blends in the presence of water. A good representation of the aqueous phase is very important from an environmental point of view, whereas the water solubility in the organic phase has a major impact on the physicochemical properties of the blend. Also the partition coefficient of ethanol between the organic and aqueous phases is an important property to be calculated under phase split conditions.

In this case, the GCA-EoS equation was only able to qualitatively predict the partition coefficient and binodal curve of the ternary cyclohexane + water + ethanol system at the plait-point region, when interaction parameters optimized on binary data only were used. Similar results were previously found with alkanes (normal [24] and branched [20]) and aromatic hydrocarbons [19]. For this reason, experimental data on this ternary system at 293 K [39] and 323 K [40] were included in the optimization procedure, as reported in Table 3. The GCA-EoS correlation and prediction of binodal curves and partition coefficients are shown in Figs. 8 and 9, respectively.

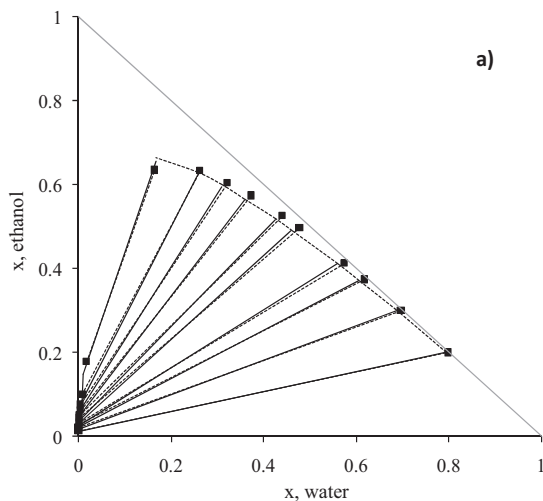


Fig. 8. Water (1)+ethanol (2)+cyclohexane (3) ternary system at 293 (a) and 313 K (b) and atmospheric pressure. Experimental data: [39,67] (points and solid lines). Dashed lines in (a) and (b): GCA-EoS correlations and predictions, respectively.

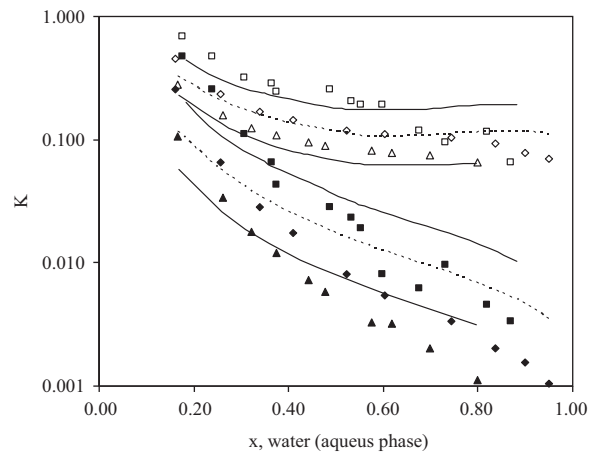


Fig. 9. Ethanol + water + cyclohexane ternary system. Ethanol and water partition coefficients at (▲,△) 293 K, (♦,◊) 308 K and (■,□) 323 K and atmospheric pressure. Open symbols: ethanol partition coefficient. Full symbols: water partition coefficient. Experimental data: [39,40]. Solid lines: GCA-EoS correlation. Dashed lines: GCA-EoS predictions.

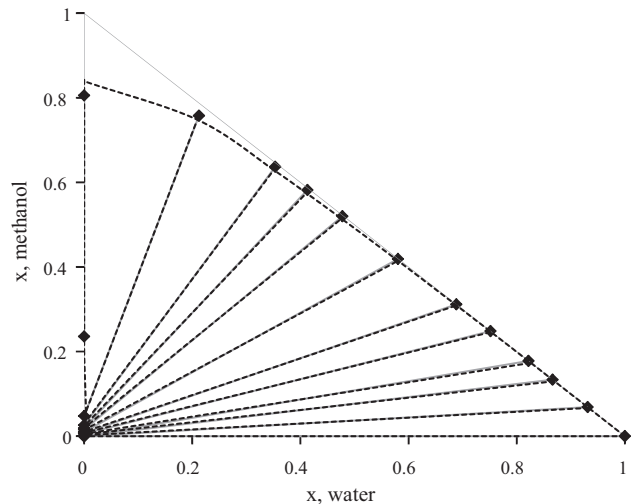


Fig. 10. Water (1)+methanol (2)+cyclohexane (3) ternary system at 303 K and atmospheric pressure. Experimental data [65] (points and solid lines). Dashed lines: GCA-EoS predictions.

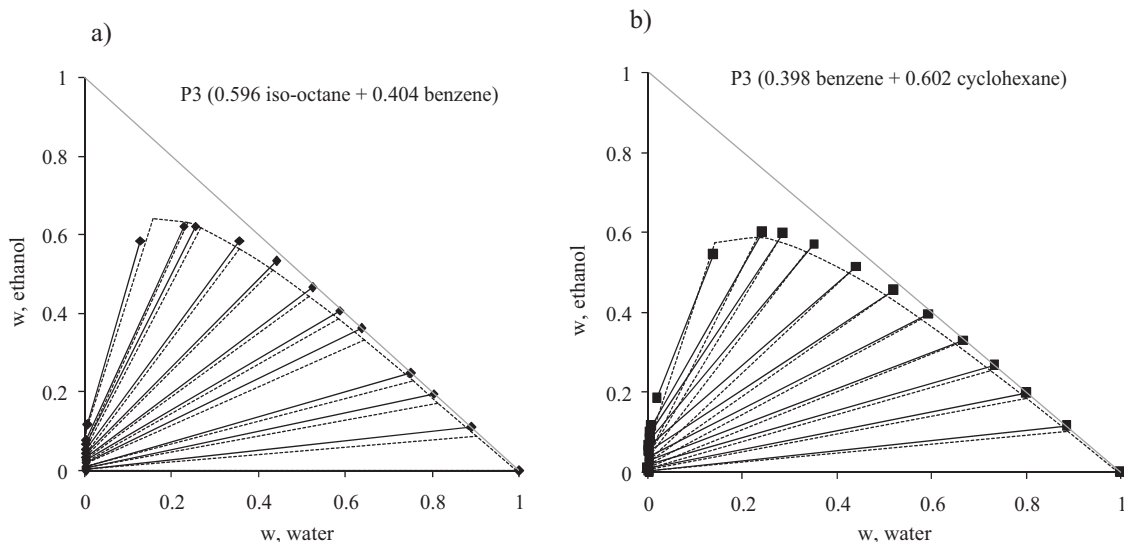


Fig. 11. Quaternary systems ethanol + benzene + water+: (a) iso-octane and (b) cyclohexane at 303 K and atmospheric pressure. Experimental data [64,69]: (dots and solid tie lines). Dashed lines: GCA-EoS predictions.

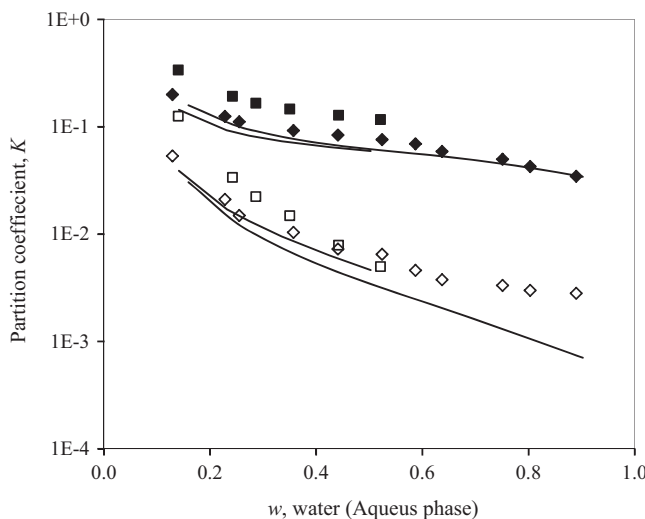


Fig. 12. Ethanol and water partition coefficients at 303 K and atmospheric pressure in the quaternary system ethanol + water + benzene+: (\diamond) iso-octane and (\square) cyclohexane. Experimental data [64,69]: Open symbols: water partition coefficients. Full symbols: ethanol partition coefficients. Solid Lines: GCA-EoS predictions.

In addition, the LLE of the methanol + water + cyclohexane ternary system at 303.15 K was predicted. Good agreement with the data measured by Gramajo de Doz et al. [65] was obtained, as shown in Fig. 10.

4.4. Phase equilibria of multicomponent systems including cyclic compounds

Gramajo de Doz et al. [64–66,68–70] carried on an extensive experimental study with quaternary mixtures containing alcohols (methanol, ethanol), water and hydrocarbons (aliphatic and aromatic). The authors used this data to analyze the water tolerance of different blends, assessing the effect of different components on the phase separation of the mixture. Alcohol affinity for water causes a reduction of the concentration of this biofuel in the organic phase after phase split, affecting the functions (antiknock and combustion emissions) that this oxygenated additive performs in the fuel. The presence of aromatic hydrocarbons increases the water tolerance

of the fuel. On the other hand, ethanol blends have higher water tolerance than methanol blends.

Figs. 11 and 12 compare the GCA-EoS predictions with the experimental data measured by Gramajo de Doz et al. [64,69] for the quaternary systems ethanol + cyclohexane + benzene + water and ethanol + iso-octane + benzene + water. The model gives a good prediction of the binodal curve and partition coefficients of water and ethanol between the organic and aqueous phases. It is important to highlight that in this case the prediction of partition coefficients is a hard test for the model, because this quantity is the ratio between two small concentrations, due to the high immiscibility of the systems.

5. Conclusions

Knowledge on the phase behavior of mixtures containing gasoline, ethanol and water is required to predict the properties of bioethanol/gasoline blends. Moreover, other alcohols such as butanol can be used as oxygenated fuel additive. Since a gasoline is a mixture of many hydrocarbons, the use of a group contribution approach to model the phase behavior reduces greatly the number of parameters required to account for the interaction between the different components. In previous work, the group contribution with association equation of state (GCA-EoS) was revised to predict the phase behavior of mixtures containing alkanes (normal [24], branched [20]) and aromatic hydrocarbons [19] with water and alcohols. In this work we have upgraded the GCA-EoS equation to work with mixtures containing also cycloalkanes. The model is now under conditions to predict properties of alcohol/gasoline blends, such as Reid vapor pressures, distillation curves and water tolerance. The model extension to cyclic compounds required a revision of the way the surface area of cyclic functional groups is calculated. The traditional simplification applied in group-contribution models, did not allow an adequate representation of the different members of the same family. The revised GCA-EoS table of parameters allowed accurate predictions of VLE and LLE phase behavior in multicomponent mixtures.

List of symbols

A Helmholtz free energy.

A_{vdW}	Van der Waals relative area.
$\text{AAD}(Z)$	average absolute deviation in variable Z:
	$\frac{1}{N} \sum_i^N Z_{i,\text{exp}} - Z_{i,\text{calc}} $
$\text{ARD}(Z)\%$	average relative deviation in variable Z:
	$\frac{100}{N} \sum_i^N \left \frac{Z_{i,\text{exp}} - Z_{i,\text{calc}}}{Z_{i,\text{exp}}} \right $
CN	carbon number
d_i	effective hard sphere diameter of component i .
d_{ci}	effective hard sphere diameter of component i evaluated at T_c .
g_j	group energy per surface segment of group j .
LLE	liquid–liquid equilibria.
N	number of experimental points of each data set.
NC	number of components in the mixture.
NG	number of attractive groups in the mixture.
NGA	number of associating groups in the mixture.
P	pressure.
q_j	number of surface segments of group j .
R	universal gas constant.
T	temperature.
T_{ci}	critical temperature of component i .
V	total volume of the mixture.
VLE	vapor–liquid equilibria.
w_i	mass composition of component i .
X_{ki}	fraction of non-bonded associating sites of type k in group i .
x_i	molar composition in liquid phase of component i .
y_i	molar composition in vapor phase of component i .
Z	dummy variable.
z	coordination number.

Greek symbols

α_{ij}	non-randomness parameter between groups i and j .
$\Delta Z\%$	ARD% in variable Z .
$\varepsilon_{ki,lj}$	energy of association between site k of group i and site l of group j .
$\kappa_{ki,lj}$	volume of association between site k of group i and site l of group j .
v_{ij}	number of groups j in compound i .
v_{ij}^*	number of associating groups j in compound i .

Acknowledgments

The authors are grateful to CONICET, ANPCyT and Universidad Nacional del Sur for the financial support.

Appendix A. Appendix: GCA-EoS mathematical model

There are three contributions to the residual Helmholtz energy in the GCA-EoS model: free volume, attractive and associating. The free volume and attractive contributions are based on Carnahan–Starling and NRTL models respectively, and keep the same form as the original GC-EoS Skjøld–Jorgensen equation [17].

The Carnahan–Starling repulsive term follows the expression developed by Mansoori and Leland [18]:

$$\frac{A^{\text{fv}}}{RT} = 3 \frac{\lambda_1 \lambda_2}{\lambda_3} (Y - 1) + \frac{\lambda_2^3}{\lambda_3^2} (Y^2 - Y - \ln Y) + n \ln Y \quad (\text{A.1})$$

with

$$Y = \left(1 - \frac{\pi \lambda_3}{6V} \right)^{-1} \quad (\text{A.2})$$

$$\lambda_k = \sum_j^{NC} n_j d_j^k \quad (\text{A.3})$$

where n_i is the number of moles of component i , NC stands for the number of components, V represents the total volume, R stands for universal gas constant and T is temperature.

The following generalized expression is assumed for the hard sphere diameter temperature dependence:

$$d_i = 1.065655 d_{ci} \left[1 - 0.12 \exp \left(- \frac{2T_{ci}}{3T} \right) \right] \quad (\text{A.4})$$

where d_c is the value of the hard sphere diameter at the critical temperature, T_c , for the pure component.

The attractive contribution to the residual Helmholtz energy (A^{att}) accounts for dispersive forces between functional groups. It is a van der Waals type contribution combined with a density-dependent, local-composition expression based on a group contribution version of the NRTL model. Integrating van der Waals EoS, $A^{\text{att}}(T,V)$ is equal to $-a \cdot n \cdot \rho$ with a the energy parameter, n the number of moles and ρ the mol density. For a pure component a is computed as follows:

$$a = \frac{z}{2} q^2 g(T) \quad (\text{A.5})$$

where g is the characteristic attractive energy per segment and q is the surface segment area per mole as defined in the UNIFAC method. The interactions are assumed to take place through the surface and the coordination number z is set equal 10 as usual. In GCA-EoS the extension to mixtures is carried out using the two fluids model NRTL model, but using local surface fractions like in UNIQUAC rather than local mole fractions. Therefore, the A^{att} for the mixture becomes

$$\frac{A^{\text{att}}}{RT} = - \frac{\frac{z}{2} \tilde{q} g_{\text{mix}}(T, V)}{RTV} \quad (\text{A.6})$$

where \tilde{q} is the total number of surface segments and g_{mix} the mixture characteristic attractive energy per total segments and are calculated as follows:

$$g_{\text{mix}} \sum_{j=1}^{NG} \theta_j \sum_{k=1}^{NG} \frac{\theta_k g_{kj} \tau_{kj}}{\sum_{l=1}^{NG} \theta_l \tau_{lj}} \quad (\text{A.7})$$

and

$$\tilde{q} = \sum_{i=1}^{NC} \sum_{j=1}^{NG} n_i v_{ij} q_j \quad (\text{A.8})$$

where v_{ij} is the number of groups of type j in molecule i ; q_j stands for the number of surface segments assigned to group j ; θ_k represents the surface fraction of group k ;

$$\theta_j = \frac{q_j}{\tilde{q}} \sum_{i=1}^{NC} n_i v_{ij} \quad (\text{A.9})$$

$$\tau_{ij} = \exp \left(\frac{\alpha_{ij} \Delta g_{ij} \tilde{q}}{RTV} \right) \quad (\text{A.10})$$

$$\Delta g_{ij} = g_{ij} - g_{jj} \quad (\text{A.11})$$

g_{ij} stands for the attractive energy between groups i and j ; and α_{ij} is the non-randomness parameter. The attractive energy between unlike groups is calculated from the corresponding interactions between like groups:

$$g_{ij} = k_{ij}^* \sqrt{g_{ii} g_{jj}} \quad (k_{ij} = k_{ji}) \quad (\text{A.12})$$

with the following temperature dependence for the energy and interaction parameters:

$$g_{ii} = g_i^* \left[1 + g_i' \left(\frac{T}{T_i^*} - 1 \right) + g_i'' \ln \left(\frac{T}{T_i^*} \right) \right] \quad (\text{A.13})$$

and

$$k_{ij} = k_{ij}^* \left[1 + k_{ij}' \ln \left(\frac{2T}{T_i^* + T_j^*} \right) \right] \quad (\text{A.14})$$

where g_i^* is the attractive energy and k_{ij}^* the interaction parameter at the reference temperature T_i^* and $(T_i^* + T_j^*)/2$, respectively.

The associating term A^{assoc} follows Wertheim's first order perturbation theory through a group-contribution expression [16]:

$$\frac{A^{\text{assoc}}}{RT} = \sum_{i=1}^{\text{NGA}} n_i^* \left[\sum_{k=1}^{M_i} \left(\ln X_{ki} - \frac{X_{ki}}{2} \right) + \frac{M_i}{2} \right] \quad (\text{A.15})$$

In this equation NGA represents the number of associating functional groups, n_i^* the total number of moles of associating group i , X_{ki} the fraction of group i non-bonded through site k and M_i the number of associating sites in group i . The total number of moles of associating group i is calculated from the number v_{mi}^* of associating groups i present in molecule m and the total amount of moles of specie m (n_m):

$$n_i^* = \sum_{m=1}^{NC} v_{mi}^* n_m \quad (\text{A.16})$$

The fraction of groups i non-bonded through site k is determined by the expression:

$$X_{ki} = \left(1 + \sum_{j=1}^{\text{NGA}} \sum_{l=1}^{M_j} \frac{n_j^* X_{kj} \Delta_{kj, jl}}{V} \right)^{-1} \quad (\text{A.17})$$

where the summation includes all NGA associating groups and M_j sites. X_{ki} depends on the association strength $\Delta_{kj, jl}$:

$$\Delta_{kj, jl} = \kappa_{kj, jl} \left[\exp \left(\frac{\varepsilon_{kj, jl}}{T} \right) - 1 \right] \quad (\text{A.18})$$

The association strength between site k of group i and site l of group j depends on the temperature T and on the association parameters $\kappa_{kj, jl}$ and $\varepsilon_{kj, jl}$, which represent the volume and energy of association, respectively.

References

- [1] E.L. Eliel, S.H. Wilen, L.N. Mander, Stereochemistry of Organic Compounds, 1st ed., J. Wiley & Sons, New York, 1994.
- [2] M. Wertheim, J. Stat. Phys. 35 (1984) 19–47.
- [3] H. Huang, M. Radosz, Ind. Eng. Chem. Res. 30 (1991) 1994–2005.
- [4] S. Suresh, J.R. Elliott, Ind. Eng. Chem. Res. 31 (1992) 2783–2794.
- [5] I. Economou, M. Donohue, Ind. Eng. Chem. Res. 31 (1992) 2388–2394.
- [6] B.J. Gross, G. Sadowski, Ind. Eng. Chem. Res. 41 (2002) 5510–5515.
- [7] A. Grenner, G. Kontogeorgis, N. von Solms, M. Michelsen, Fluid Phase Equilib. 258 (2007) 83–94.
- [8] C. Coquelet, C.-B. Soo, A. Valtz, D. Richon, D. Amorosc, H. Gayet, Fluid Phase Equilib. 298 (2010) 33–37.
- [9] I.V. Yakoumis, G.M. Kontogeorgis, E.C. Voutsas, D.P. Tassios, Fluid Phase Equilib. 130 (1997) 31–47.
- [10] E.C. Voutsas, G.M. Kontogeorgis, I.V. Yakoumis, D.P. Tassios, Fluid Phase Equilib. 132 (1997) 61–75.
- [11] G.K. Folas, S.O. Derawi, M.L. Michelsen, E.H. Stenby, G.M. Kontogeorgis, Fluid Phase Equilib. 228–229 (2005) 121–126.
- [12] I.V. Yakoumis, G.M. Kontogeorgis, E.C. Voutsas, E.M. Hendriks, D.P. Tassios, Ind. Eng. Chem. Res. 37 (1998) 4175–4182.
- [13] A. Grenner, I. Tsivintzelis, I. Economou, C. Panayiotou, G. Kontogeorgis, Ind. Eng. Chem. Res. 47 (2008) 5636–5650.
- [14] I. Tsivintzelis, A. Grenner, I. Economou, G. Kontogeorgis, Ind. Eng. Chem. Res. 47 (2008) 5651–5659.
- [15] M.S. Zabaloy, G.D.B. Mabe, S.B. Bottini, E.A. Brignole, Fluid Phase Equilib. 83 (1993) 159–166.
- [16] H.P. Gros, S.B. Bottini, E.A. Brignole, Fluid Phase Equilib. 116 (1996) 537–544.
- [17] S. Skjold-Jørgensen, Ind. Eng. Chem. Res. 27 (1988) 110–118.
- [18] G.A. Mansoori, T.W. Leland Jr., J. Chem. Soc. Faraday Trans. 68 (1972) 320–344.
- [19] F.A. Sánchez, S. Pereda, E.A. Brignole, Fluid Phase Equilib. 306 (2011) 112–123.
- [20] T.M. Soria, A.E. Andreatta, S. Pereda, S.B. Bottini, Fluid Phase Equilib. 302 (2011) 1–9.
- [21] A.J. Bondi, Phys. Chem. 68 (1964) 441–451.
- [22] M.S. Gordon Quantum Theory Group, Ames Laboratory, Iowa State University, <http://www.msg.ameslab.gov/gamess>
- [23] Project 801, Evaluated Process Design Data, Public Release Documentation; Design Institute for Physical Properties (DIPPR), American Institute of Chemical Engineers (AIChE), New York, 2006.
- [24] T.M. Soria, F.A. Sánchez, S. Pereda, S.B. Bottini, Fluid Phase Equilib. 296 (2010) 116–124.
- [25] J. Chevalley, Comp. Rend. 250 (1960) 3326–3328 (Dechema Chemistry Data Series, vol. 1, part 2b).
- [26] R.M. Stephenson, J. Stuart, J. Chem. Eng. Data 31 (1986) 56–70.
- [27] C. Marche, C. Ferronato, J.-C. De Hemptinne, J. Jose, J. Chem. Eng. Data 51 (2006) 355–359.
- [28] C. Marche, C. Ferronato, J. Jose, J. Chem. Eng. Data 49 (2004) 937–940.
- [29] P. Dohanyosova, S. Sarraute, V. Dohnal, V. Majer, M. Costa Gomes, Ind. Eng. Chem. Res. 43 (2004) 2805–2815.
- [30] J.L. Heidman, C. Tsonopoulos, C.J. Brady, G.M. Wilson, AIChE J. 31 (1985) 376–384.
- [31] A. Maczynski, B. Wisniewska-Gocłowska, M. Góral, J. Phys. Chem. Ref. Data 33 (2004) 549–577.
- [32] R.W. Kiser, G.D. Johnson, M.D. Sheltar, J. Chem. Eng. Data 6 (1961) 338–341.
- [33] D.C. Jones, S. Amstell, J. Chem. Soc. (1930) 1316–1323 (Dechema Chemistry Data Series, vol. 1, part 1).
- [34] E.L. Eckfeldt, W.W. Lucasse, J. Phys. Chem. 47 (1943) 164–183 (Dechema Chemistry Data Series, vol. 1, part 1).
- [35] N. Isii, J. Soc. Chem. Ind. Jap. 38 (1935) 659–664 (Dechema Chemistry Data Series, vol. 1, part 2c).
- [36] C.B. Kretschmer, R. Wiebe, J. Am. Chem. Soc. 71 (1949) 3176–3179 (Dechema Chemistry Data Series, vol. 1, part 2c).
- [37] J. Nagai, N. Isii, J. Soc. Chem. Ind. Jap. 38 (1935) 86–95 (Dechema Chemistry Data Series, vol. 1, part 2c).
- [38] G. Scatchard, F.G. Satkiewicz, J. Am. Chem. Soc. 86 (1964) 130–133 (Dechema Chemistry Data Series, vol. 1, part 2c).
- [39] C.-Y. Huang, P.-Y. Chung, I.-M. Tseng, L.-S. Lee, Open Thermodyn. J. 4 (2010) 102–118.
- [40] M. Antosik, M. Gałka, S.K. Malanowski, J. Chem. Eng. Data 49 (2004) 7–10.
- [41] B.N. Raju, D.P. Rao, J. Chem. Eng. Data 14 (1969) 283–286.
- [42] J. Ocon, G. Tojo, M. Bao, A. Arce, An. Real. Soc. Espan. De Fis. y Quim. 69 (1973) 1169–1176.
- [43] K. Strubl, V. Svoboda, R. Holub, J. Pick, Collect. Czech. Chem. Commun. 35 (1970) 3004–3019 (Dechema Chemistry Data Series, vol. 1, part 2c).
- [44] N.A. Smirnova, L.M. Kurtymina, Zh. Fiz. Khim. 43 (1969) 1883–1885.
- [45] V. Svoboda, R. Holub, J. Pick, Collect. Czech. Chem. Commun. 36 (1971) 2331–2338.
- [46] H.S. Mylers, Petrol. Refiner. 36 (1957) 175–178 (Dechema Chemistry Data Series, vol. 1, part 6b).
- [47] K. Ridgway, P.A. Butler, J. Chem. Eng. Data 12 (1967) 509–515 (Dechema Chemistry Data Series, vol. 1, part 6b).
- [48] M.P. Suserev, S.T. Chen, Zh. Fiz. Khim. 37 (1963) 1739–1744 (Dechema Chemistry Data Series, vol. 1, part 6b).
- [49] W.E. Ehret, H.J. Weber, J. Chem. Eng. Data 4 (1959) 142–145 (Dechema Chemistry Data Series, vol. 1, part 6b).
- [50] C. Black, Ind. Eng. Chem. 51 (1959) 211 (Dechema Chemistry Data Series, vol. 1, part 6b).
- [51] J.L. Cruetzen, R. Haase, L. Sieg, Z. Naturforsch. A 5 (1950) 600–604 (Dechema Chemistry Data Series, vol. 1, part 6b).
- [52] D.V.S. Jain, O.P. Yadav, Indian J. Chem. 9 (1971) 342–345 (Dechema Chemistry Data Series, vol. 1, part 6b).
- [53] P. Oracz, M. Góral, G. Wilczek-Vera, S. Warycha, Fluid Phase Equilib. 126 (1996) 71–92.
- [54] S. Madhavan, P.S. Murti, Chem. Eng. Sci. 21 (1966) 465–468.
- [55] O. Vilim, Collect. Czech. Chem. Commun. 26 (1961) 2124–2133 (Dechema Chemistry Data Series, vol. 1, part 2a).
- [56] A.G. Morachevsky, V.T. Zharov, Zh. Prikl. Khim. 36 (1963) 2771 (Dechema Chemistry Data Series, vol. 1, part 2c).
- [57] K.S. Yuan, B.C-Y. Lu, J.C.K. Ho, A.K. Keshpande, J. Chem. Eng. Data 8 (1963) 549–559.
- [58] A. Verrazzi, I. Kikic, P. Garbers, A. Barreau, D. Le Roux, J. Chem. Eng. Data 43 (1998) 949–953.
- [59] J.E. Sinor, J.H. Weber, J. Chem. Eng. Data 5 (1960) 243–247.
- [60] D.E.G. Jones, I.A. Weeks, S.C. Anand, R.W. Wetmore, G.C. Benson, J. Chem. Eng. Data 17 (1972) 501–506.
- [61] G.C. Benson, S.C. Anand, O. Kiyohara, J. Chem. Eng. Data 19 (1974) 258–261.
- [62] S.C. Anand, J.-P.E. Golier, O. Kiyohara, C.J. Halpin, G.C. Benson, J. Chem. Eng. Data 20 (1975) 184–189.
- [63] B.A. Englin, A.F. Plate, V.M. Tugolukov, M.A. Pryanishnikova, Khim. Tekhnol. Topl. Masel. 10 (1965) 42–46.

- [64] M.B. Gramajo de Doz, C.M. Bonatti, H.N. Sólamo, *J. Chem. Thermodyn.* 35 (2003) 2055–2065.
- [65] M.B. Gramajo de Doz, C.M. Bonatti, H.N. Sólamo, *J. Chem. Thermodyn.* 35 (2003) 825–837.
- [66] M.B. Gramajo de Doz, C.M. Bonatti, H.N. Sólamo, *Fluid Phase Equilib.* 205 (2003) 53–67.
- [67] R.M. Stephenson, *J. Chem. Eng. Data* 37 (1992) 80–95.
- [68] M.B. Gramajo de Doz, C.M. Bonatti, N. Barnes, H.N. Sólamo, *J. Chem. Thermodyn.* 33 (2001) 1663–1677.
- [69] M.B. Gramajo de Doz, C.M. Bonatti, N. Barnes, H.N. Sólamo, *Sep. Sci. Technol.* 37 (2002) 245–260.
- [70] M.B. Gramajo de Doz, C.M. Bonatti, H.N. Sólamo, *Fluid Phase Equilib.* 230 (2005) 45–50.